

# Supporting Information

## Degradation of Aqueous Polycyclic Musk Tonalide by Ultraviolet-Activated Free Chlorine

Lili Wang <sup>1,\*</sup> and Xiaowei Liu <sup>2,3,\*</sup>

<sup>1</sup> Environmental Engineering, Jiyang College of Zhejiang A & F University, Zhuji 311800, PR China; lililive@163.com

<sup>2</sup> Institute of Water Resources & Ocean Engineering, Ocean College, Zhejiang University, Hangzhou 310058, PR China; liuxiaowei@zju.edu.cn

<sup>3</sup> Institute of Municipal Engineering, College of Civil Engineering and Architecture, Zhejiang University, Hangzhou 310058, PR China

\* Correspondence: lililiwang@zafu.edu.cn liuxiaowei@zju.edu.cn; Tel.: +86-571-88208721

### Section S1. Determination of effective optical path length

The direct photolysis of dilute H<sub>2</sub>O<sub>2</sub> by UV irradiation at 254 nm can be expressed as the following equation (Equation (1)):

$$d[\text{H}_2\text{O}_2]/dt = -2.3\varepsilon L\Phi_p I_0 [\text{H}_2\text{O}_2] = -k_{\text{obs}} [\text{H}_2\text{O}_2] \quad (1)$$

where  $I_0$  represents the photon flux (Einstein sec<sup>-1</sup>),  $\varepsilon_{\text{H}_2\text{O}_2}$  is the molar extinction coefficient of H<sub>2</sub>O<sub>2</sub> (M<sup>-1</sup>·cm<sup>-1</sup>),  $L$  is the effective light path length (cm),  $\Phi_p$  is the quantum yield of photolysis of H<sub>2</sub>O<sub>2</sub> (mol·Einstein<sup>-1</sup>), and  $[\text{H}_2\text{O}_2]$  is the concentration of H<sub>2</sub>O<sub>2</sub> (M) at time  $t$ .

Figure S3 shows the photolysis kinetics of H<sub>2</sub>O<sub>2</sub>, and  $k_{\text{obs}}$  is the slope of the regression line, which is a function of  $\Phi_p$ ,  $\varepsilon_{\text{H}_2\text{O}_2}$ ,  $I_0$  and  $L$ . Thus, for given values of  $\Phi_p$  (1.0 mol·Einstein<sup>-1</sup>, [1]),  $\varepsilon_{\text{H}_2\text{O}_2}$  (19.6 M<sup>-1</sup>·cm<sup>-1</sup>, [2]) and  $I_0$ ,  $L$  can be easily computed from the value of  $k_{\text{obs}}$ . For the experimental reactor, the effective path length  $L$  of the photoreactor was determined to be 7.03 cm.

### Section S2. Determination of $k(\text{HO}\cdot + \text{AHTN})$ and $k(\text{RCS} + \text{AHTN})$

HO $\cdot$  was generated by peroxydisulfate activation using 1 mM KOH. 10  $\mu\text{M}$  isopropanol was added to clean formed HO $\cdot$  when PMS oxidation of AHTN and NB was tested. Because AHTN/NB decomposition caused by PMS oxidation at 3-min reaction time can be ignored (<5%, Figure S4), HO $\cdot$  was considered as the only species responsible for AHTN and NB degradation. The kinetic expression of AHTN degradation can be expressed as Equation (2) and its integrated form Equation (3):

$$-\frac{d[\text{AHTN}]}{dt} = k(\text{HO}\cdot + \text{AHTN})[\text{AHTN}][\text{HO}\cdot] \quad (2)$$

$$-\ln \frac{[\text{AHTN}]}{[\text{AHTN}]_0} = k(\text{HO}\cdot + \text{AHTN}) \int [\text{HO}\cdot] dt \quad (3)$$

where  $k(\text{HO}\cdot + \text{AHTN})$  is the second-order rate constant of AHTN with HO $\cdot$ ,  $[\text{HO}\cdot]$  is defined as the concentration of HO $\cdot$ ,  $[\text{AHTN}]_0$  and  $[\text{AHTN}]$  are the initial concentration of AHTN and concentration at time  $t$ , respectively.

Applying Equation (2) to probe compound (NB) coexisting with NB in the system, Equation (4) is obtained:

$$-\ln \frac{[\text{NB}]}{[\text{NB}]_0} = k(\text{HO}\cdot + \text{NB}) \int [\text{HO}\cdot] dt \quad (4)$$

Dividing Equation (3) with Equation (4), leads to:

$$\frac{-\ln([AHTN]/[AHTN]_0)}{-\ln([NB]/[NB]_0)} = \frac{k(HO\bullet + AHTN)}{k(HO\bullet + NB)} \quad (5)$$

Based on the reported value of  $k(HO\bullet + NB)$  ( $3.9 \times 10^9 \text{ M}^{-1}\cdot\text{s}^{-1}$ , [3]) and slope of the plot of  $-\ln([AHTN]/[AHTN]_0)$  vs.  $-\ln([NB]/[NB]_0)$  ( $k = 2.12$ , Figure S5),  $k(HO\bullet + AHTN)$  was found to be  $8.3 \times 10^9 \text{ M}^{-1}\cdot\text{s}^{-1}$ .

The steady-state concentration of  $Cl\bullet$  ( $[Cl\bullet]_{ss}$ ) was determined using competition kinetic method. In a solution containing NB, benzoic acid (BA) and AHTN, the amount of chlorine atom could be calculated based on the degradation of BA (Equation (6)) subtracting the contribution of  $HO\bullet$  (expressed in Equation (4)). Subsequently, applying the value of  $k(HO\bullet + AHTN)$  ( $8.3 \times 10^9 \text{ M}^{-1}\cdot\text{s}^{-1}$ ),  $k(HO\bullet + NB)$  ( $3.9 \times 10^9 \text{ M}^{-1}\cdot\text{s}^{-1}$ ),  $k(HO\bullet + BA)$  ( $5.9 \times 10^9 \text{ M}^{-1}\cdot\text{s}^{-1}$ , [5]), and  $k(Cl\bullet + BA)$  ( $1.8 \times 10^{10} \text{ M}^{-1}\cdot\text{s}^{-1}$ , [5]),  $[Cl\bullet]_{ss}$  was determined using Equation (7) to be  $2.8 \times 10^{-15} \text{ M}$  ( $k(Cl\bullet + BA) [Cl\bullet]_{ss} = 5.0329 \times 10^{-5}$ , Figure S6).

$$-\ln \frac{[BA]}{[BA]_0} = k(HO\bullet + BA) \int [HO\bullet] dt + k(Cl\bullet + BA) \int [Cl\bullet] dt \quad (6)$$

$$\frac{k(HO\bullet + BA)}{k(HO\bullet + NB)} \ln \frac{[NB]}{[NB]_0} - \ln \frac{[BA]}{[BA]_0} = k(Cl\bullet + BA) [Cl\bullet]_{ss} t \quad (7)$$

The second-rate of constant between AHTN and  $ClO\bullet$  ( $k(ClO\bullet + AHTN)$ ) was determined using 2,5-dimethoxybenzoate (DMBA) as reference compounds, which react with  $ClO\bullet$  at second-order rate constants of  $7.0 \times 10^8$  [4]. To create a  $ClO\bullet$ -dominated system, the UV/chlorine process was carried out at a chlorine dosage of  $50 \mu\text{M}$  and pH 8.4, and the solution was spiked with  $0.5 \text{ mM}$  tert-Butanol to scavenge the  $HO\bullet$  and  $Cl\bullet$  in the system. And  $ClO\bullet$  was the survived radical.  $k(ClO\bullet + AHTN)$  was determined using to be  $6.3 \times 10^9 \text{ M}^{-1}\cdot\text{s}^{-1}$  ( $k(ClO\bullet + AHTN)/k(ClO\bullet + DMBA) = 8.95$ , Figure S7).

### Section S3. Determination of $\epsilon_{AHTN,254}$ and $\Phi_{AHTN,254}$

The molar extinction coefficient of AHTN at 254nm was determined on the basis of Lambert-Beer's Law. Five samples of AHTN at different concentration ( $0.1 \text{ mg}\cdot\text{L}^{-1}$ ,  $0.6 \text{ mg}\cdot\text{L}^{-1}$ ,  $0.8 \text{ mg}\cdot\text{L}^{-1}$ , and  $1.0 \text{ mg}\cdot\text{L}^{-1}$ ) were prepared. Absorbance of these samples at 254 nm ( $A_{254}$ ) was analyzed with a 1 cm colorimetric dish ( $b = 1 \text{ cm}$ ).  $A_{254}$  is linearly correlated with  $\epsilon_{AHTN,254}$  according to Lambert-Beer's Law. When  $A_{254}$  was plotted against concentration of AHTN, a linear line was obtained with slope  $k = \epsilon_{AHTN,254} \times b$  (Figure S8). Finally,  $\epsilon_{AHTN,254}$  was calculated to be  $13583 \text{ M}^{-1}\cdot\text{cm}^{-1}$ . Quantum yield of AHTN at 254 nm ( $\Phi_{AHTN,254}$ ) was determined by plotting degraded amount of AHTN against absorbed photon (photo flux  $\times$  irradiation time) (Figure S9). According to the definition, the slope of the fitting line is equal to  $\Phi_{AHTN,254}$  ( $0.036 \text{ molar}\cdot\text{Einstein}^{-1}$ ).

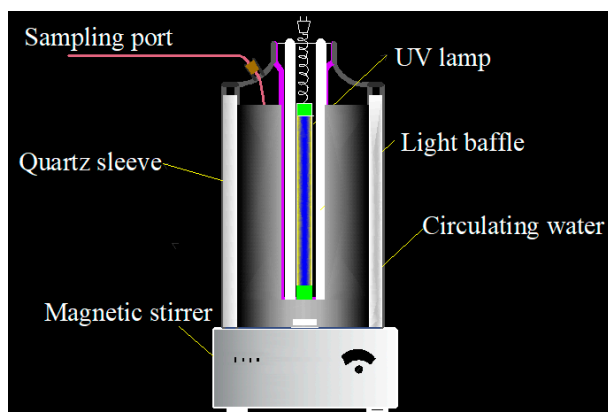
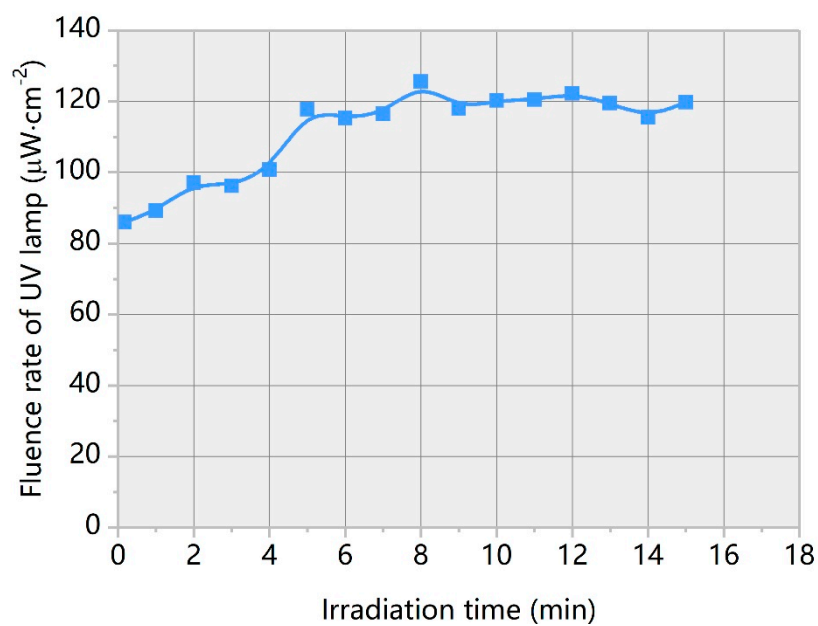
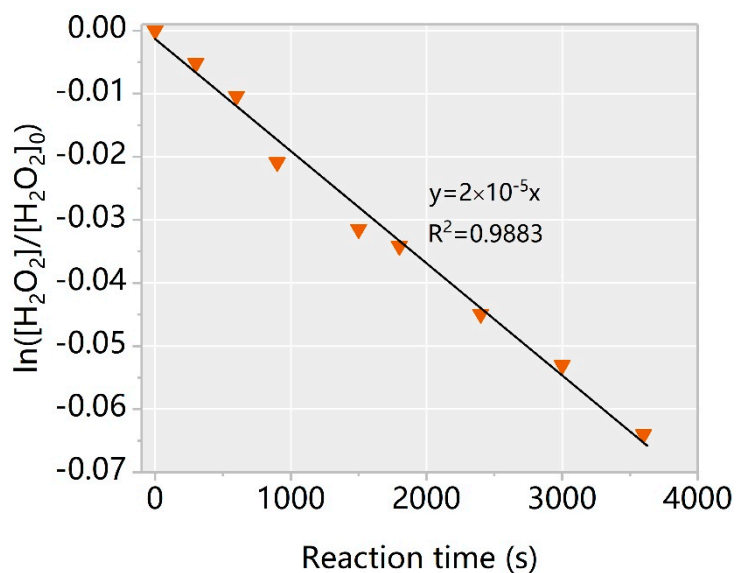


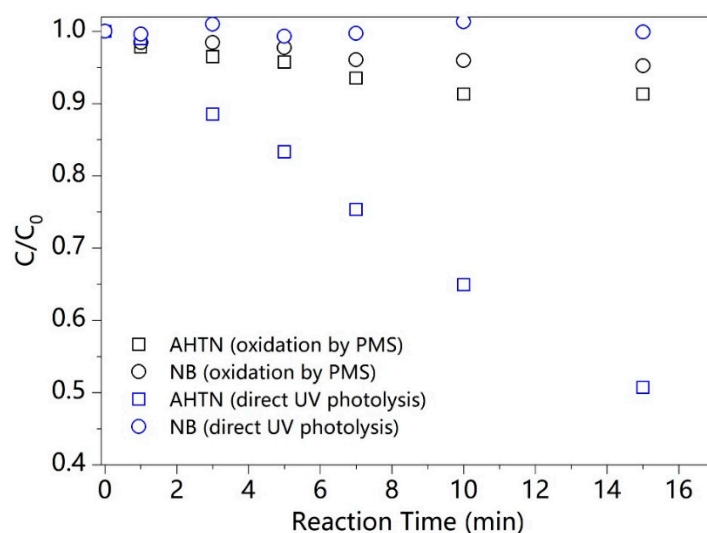
Figure S1. Set-up and construction of photoreactor



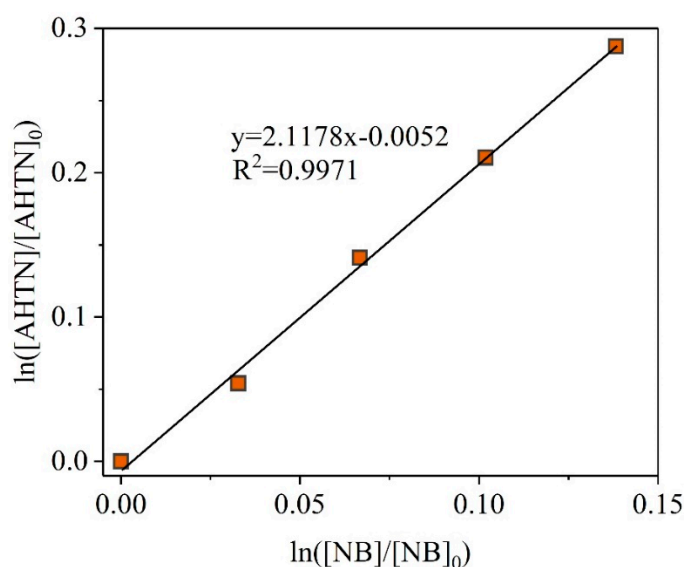
**Figure S2.** Energy output profile of UV lamp



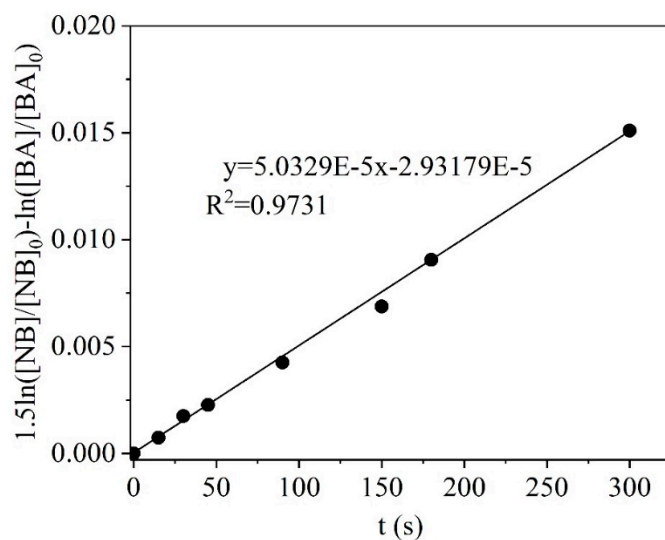
**Figure S3.** UV Photolysis of H<sub>2</sub>O<sub>2</sub> ([H<sub>2</sub>O<sub>2</sub>]<sub>0</sub> = 0.1 mM, pH = 7.0, and 25±1 °C).



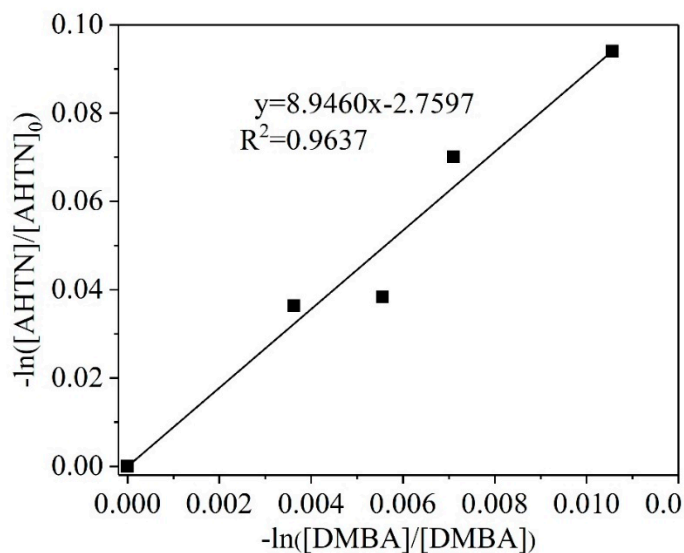
**Figure S4.** Degradation of AHTN and NB by (a) PMS oxidation in presence of 10  $\mu\text{M}$  isopropanol and (b) direct UV photolysis ( $[\text{AHTN}]_0 = 1.0 \text{ mg}\cdot\text{L}^{-1}$ ,  $[\text{NB}]_0 = 10\mu\text{M}$ ,  $[\text{PMS}]_0 = 0.5 \text{ mM}$ , UV fluence rate  $0.067 \text{ mW}\cdot\text{cm}^{-2}$ ,  $\text{pH} = 11.0$ , and  $25\pm 1 \text{ }^\circ\text{C}$ ).



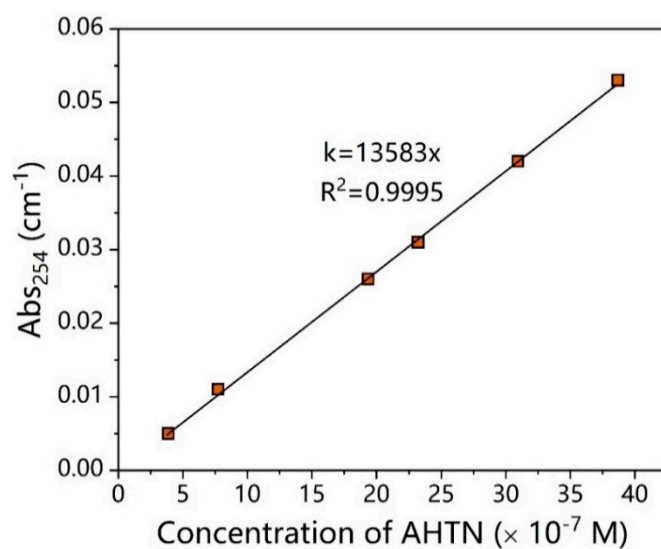
**Figure S5.**  $-\ln ([\text{AHTN}]/[\text{AHTN}]_0)$  vs  $-\ln ([\text{NB}]/[\text{NB}]_0)$  ( $[\text{AHTN}]_0 = 1.0 \text{ mg}\cdot\text{L}^{-1}$ ,  $[\text{NB}]_0 = 10\mu\text{M}$ ,  $[\text{PMS}]_0 = 0.5 \text{ mM}$ , UV fluence rate  $0.067 \text{ mW}\cdot\text{cm}^{-2}$ ,  $\text{pH} = 11.0$ , and  $25\pm 1 \text{ }^\circ\text{C}$ ).



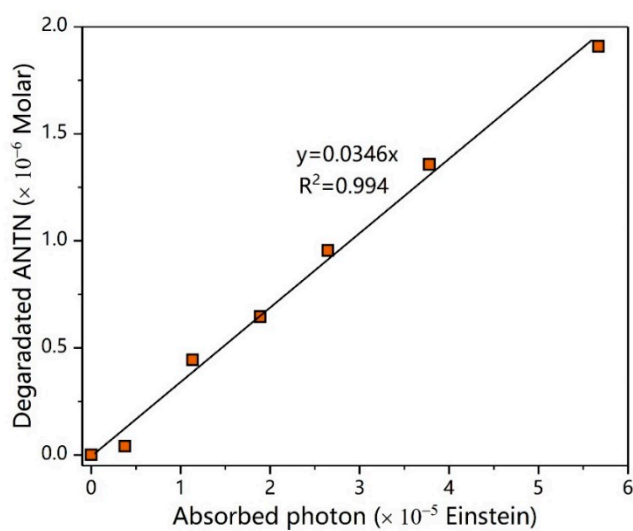
**Figure S6.**  $\left( \frac{k(\text{HO}\cdot + \text{BA})}{k(\text{HO}\cdot + \text{NB})} \ln \frac{[\text{NB}]}{[\text{NB}]_0} - \ln \frac{[\text{BA}]}{[\text{BA}]_0} \right)$  vs  $t$  ( $[\text{BA}]_0 = 0.5 \text{ mM}$ ,  $[\text{NB}]_0 = 10 \text{ }\mu\text{M}$ , UV fluence rate  $0.067 \text{ mW}\cdot\text{cm}^{-2}$ ,  $\text{pH} = 7.0$ , and  $25 \pm 1 \text{ }^\circ\text{C}$ ).



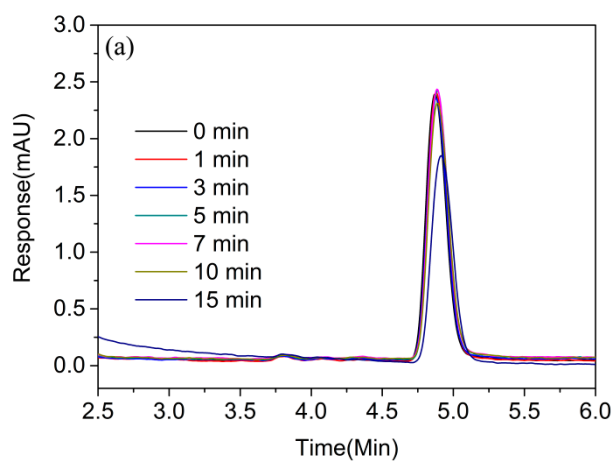
**Figure S7.** Degradation of AHTN and DMOB in the  $\text{ClO}\cdot$  system ( $[\text{AHTN}]_0 = 1.0 \text{ mg}\cdot\text{L}^{-1}$ ,  $[\text{DMBA}]_0 = 0.5 \text{ mM}$ ,  $[\text{FC}]_0 = 50 \text{ }\mu\text{M}$ ,  $\text{pH} = 8.4$ ,  $25 \pm 1 \text{ }^\circ\text{C}$ , and UV fluence rate  $= 0.067 \text{ mW}\cdot\text{cm}^{-2}$ ).

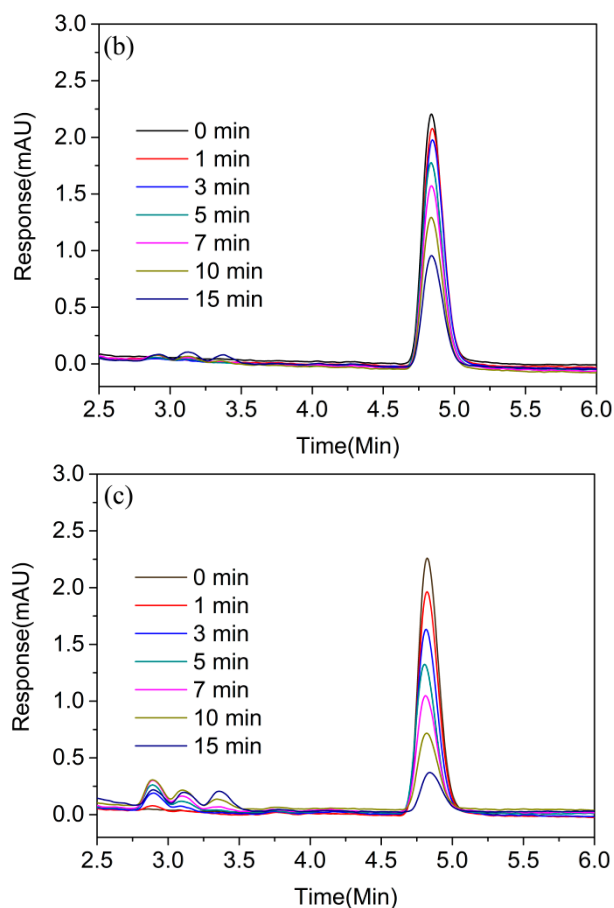


**Figure S8.** UV absorbance of AHTN at different concentration (pH = 7.0 and 25 °C)

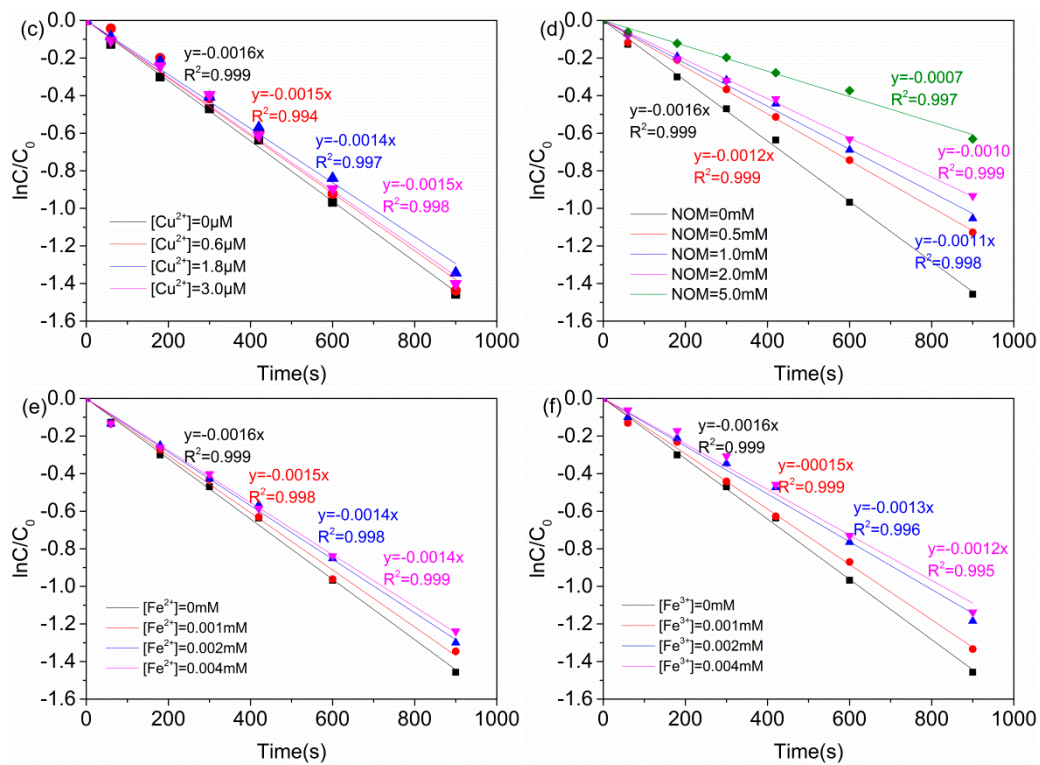


**Figure S9.** Degradation of AHTN corresponding to different absorbed photon ( $[\text{AHTN}]_0 = 1.0 \text{ mg}\cdot\text{L}^{-1}$ , pH = 7.0, photon flux  $1.67 \times 10^{-9} \text{ Einstein}\cdot\text{s}^{-1}$ , and 25 °C).





**Figure S10.** Chromatogram for HPLC of AHTN degradation by (a) FC, (b) UV, and (c) UV/FC ( $[AHTN]_0 = 1.0 \text{ mg} \cdot \text{L}^{-1}$ ,  $\text{pH} = 7.0$ ,  $25 \pm 1^\circ \text{C}$ , and  $[FC]_0 = 3.28 \text{ mg} \cdot \text{L}^{-1}$ ).





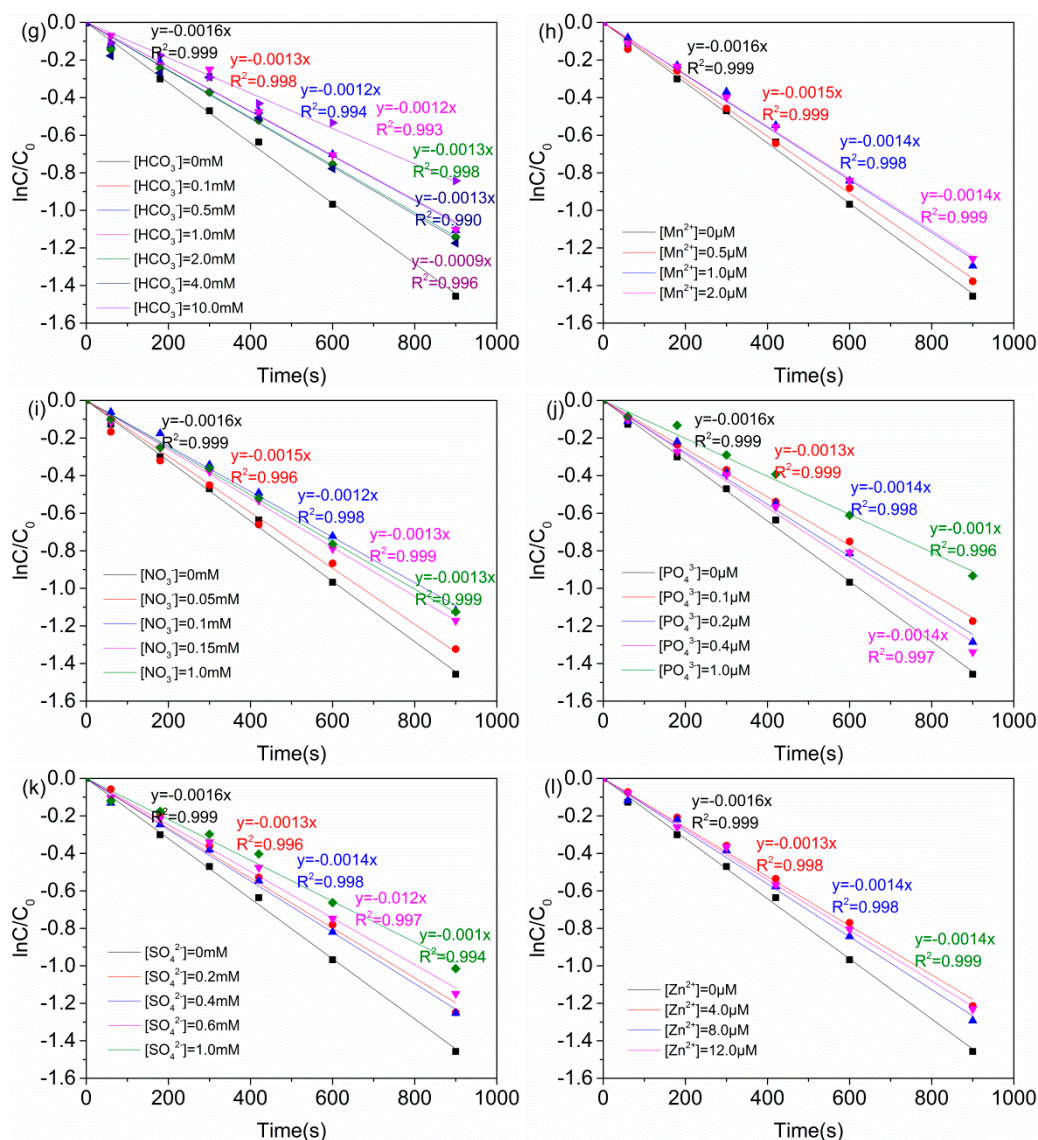


**Figure S11.** AHTN degradation by UV/FC under various conditions (Varying conditions are based on the control experiment:  $[AHTN]_0 = 1.0 \text{ mg}\cdot\text{L}^{-1}$ ,  $\text{pH} = 7.0$ ,  $25 \pm 1^\circ\text{C}$ ,  $[FC]_0 = 3.28 \text{ mg}\cdot\text{L}^{-1}$ , and UV fluence rate  $0.067 \text{ mW}\cdot\text{cm}^{-2}$ ).

**Table S1.** Method detection limits (MDL) of halogenated DBPs.

Name	MDLs ( $\mu\text{g}\cdot\text{L}^{-1}$ )
Chloroform	0.01
1,1,1-trichloroethane	0.02
1,1,2-trichloroethane	0.02
1,1-dichloro-2-propanone	0.06
1,1,1-trichloro-2-propanone	0.05
1,2,3-trichloropropane	0.01
Carbon tetrachloride	0.04
Trichloroethylene	0.02
Tetrachloroethylene	0.01
Chloralhydrate	0.03
Monochloroacetic acid	0.05
Dichloroacetic acid	0.05
Trichloroacetic acid	0.04



## References:

1. J. Baxendale, J. Wilson, The photolysis of hydrogen peroxide at high light intensities, Transactions of the Faraday Society 53 (1957) 344–356.
2. X. Liu, L. Fang, Y. Zhou, T. Zhang, Y. Shao, Comparison of UV/PDS and UV/H<sub>2</sub>O<sub>2</sub> processes for the degradation of atenolol in water, *J. Environ. Sci.* **2013**, 25, 1519–1528.
3. Y. Guan, J. Ma, X. Li, J. Fang, L. Chen, Influence of pH on the formation of sulfate and hydroxyl radicals in the UV/peroxymonosulfate system, *Environ. Sci. Technol.* **2011**, 45, 9308–9314.
4. Z.B. Alfassi, R.E. Huie, S. Mosseri, P. Neta, Kinetics of one-electron oxidation by the ClO radical, *Int. J. Rad. Appl. Instrum. C.*, **1988**, 32, 85–88.